  Bull. Chem. Soc. Jpn., 61, 1831—1836 (1988)

Crystal Structures and Electronic Properties of Organic Conductors Based on AzaTCNQ

Hatsumi URAYAMA,*,†† Tamotsu INABE, Takehiko MORI, Yusei MARUYAMA, and Gunzi SAITO†
Institute for Molecular Science, Myodaiji-cho, Okazaki, Aichi 444
†Institute for Solid State Physics, The University of Tokyo, Roppongi, Minato-ku, Tokyo 106
(Received August 7, 1987)

AzaTCNQ ((4-dicyanomethyl-1-pyridinio)dicyanomethanide) is employed as an organic acceptor to form new organic conductors with a TTF family such as TTF,[1] TMTTF, TMTSF, HMTTF, and DBTTF. Among them, TMTTF and TMTSF give 2:1 single crystals and the latter affords the most conductive complex, showing a metallic characteristic down to 150 K. This can be observed by measuring the thermoelectric power and the ESR spectra. A crystal structure analysis indicates that only TMTSF molecules stack to form one-dimensional conduction pathways, while AzaTCNQ molecules are arranged side-by-side and oriented almost perpendicular to the donor molecules. There exists an orientational disorder of the nitrogen atom in the pyridine skeletone of an AzaTCNQ molecule, which may be associated with the weak temperature dependence of the electrical conductivity.

In an attempt to develop new highly conducting organic charge-transfer complexes, a number of novel donors and acceptors have been synthesized. One of the prominent acceptors is AzaTCNQ (Fig. 1). It has a similar geometry to TCNQ. However, the electronic properties of AzaTCNQ are different from those of TCNQ since the AzaTCNQ molecule contains a pyridine skeleton instead of the quinonoid ring of the TCNQ molecule. In the neutral state the spin multiplicity of AzaTCNQ is doublet. AzaTCNQ is, however, more stable as a closed-shell anion than a neutral radical and acts as one of the strongest π-electron acceptors so far obtaind. The reduced acceptor, AzaTCNQ$^-$, can be used as an organic anion instead of inorganic anions, e.g. BF_4^-, ClO_4^-, etc.

Originally, AzaTCNQ was synthesized by Wudl in order to search for conductive neutral radical complexes.[2] He prepared TTF complexes and reported relatively low electrical resistivities of the compacted specimens (1:1 and 2:1 stoichiometries) as 30—100 Ωcm. Later, Matsubayashi et al. regarded it as being an organic anion to form simple salts with cationic species.[3] Relatively high resistivities of more than 10^5 Ωcm were obtained.

We have investigated AzaTCNQ and its complexes for the following two purposes.[4] One was to search for conductive materials based on AzaTCNQ. The other was to elucidate the electronic states of AzaTCNQ in complexes: whether AzaTCNQ could be a neutral radical, a closed-shell anion, or a partially ionized state.

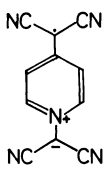

Fig. 1. Molecular structure of AzaTCNQ·.

†† Present address: The Institute for Solid State Physics, The University of Tokyo, Roppongi, Minato-ku, Tokyo 106.

In this report, we discuss the preparation of several AzaTCNQ complexes with TTF derivatives and show detailed physical and structural properties of the metallic complex $(TMTSF)_2$ AzaTCNQ.

Experimental

Microcrystals of *N*-methylpyridinium AzaTCNQ (NMPy$^+$ AzaTCNQ$^-$) were prepared by the method of Tanaka et al.[3] The product was identified by its melting point (232—233 °C, lit, 233—237 °C).[3] Black crystalline complexes with TTF were obtained by direct mixing of 0.062 g of $(TTF)_2(BF_4)_3$ in 22 ml of hot acetonitrile and 0.070 g of NMPy$^+$ AzaTCNQ$^-$ in 13 ml of the same solvent. Black shiny microcrystals of the TMTTF complex were prepared by mixing 0.056 g of $(TMTTF)_{17}(BF_4)_8$ in 40 ml of hot acetonitrile and 0.026 g of NMPy$^+$ AzaTCNQ$^-$ in 10 ml of the same solvent. Complexes with TMTTF, TMTSF, DBTTF, and HMTTF were grown electrochemically in 20 ml of 1,1,2-trichloroethane with 30 mg of NMPy$^+$ AzaTCNQ$^-$ as an electrolyte and 10 mg of donors at a constant current of 1 μA under N_2. TMTTF and TMTSF complexes were obtained as shinny black single crystals in the form of elongated rods and DBTTF and HMTTF complexes had a black polycrystalline form.

For X-ray investigations, the intensity data of the TMTSF complex were measured on a Rigaku automated four-circle diffractometer with graphite monochromated Mo$K\alpha$ radiation up to 2θ=60° by using the ω-2θ scan techniqe. The sample crystal was a black plate with dimensions of 0.08×0.25×0.60 mm^3. Then, 1214 independent reflections ($|F|>3\sigma(|F|)$) were used for a structure analysis. The structure was solved by the Patterson method and refined by the block diagonal least-squares method. Atomic scattering factors were taken from International Tables for X-ray Crystallography.[5] Cell parameters were determined from least-squares applied to 25 reflections with $27°<2\theta<31°$. The final refinement gave R=0.0548 and R_w=0.0587 for $(TMTSF)_2$ AzaTCNQ. The positional parameters are listed in Table 1. The F_o-F_c table and the anisotropic temperature parameters are deposited as Document No. 8802 at the Office of this Bulletin.

Table 1. Atomic Parameters of $(TMTSF)_2AzaTCNQ$

Atom	$X(\times10^4)$	$Y(\times10^4)$	$Z(\times10^4)$
Se(1)	5890(3)	5426(1)	3152(1)
Se(2)	5903(3)	7074(1)	3174(1)
Se(3)	6007(3)	0434(1)	3172(1)
Se(4)	5707(3)	2015(1)	3196(1)
C(1)	5466(18)	6299(12)	2807(6)
C(2)	6861(24)	6003(11)	3820(7)
C(3)	6443(26)	6594(14)	3841(9)
C(4)	7416(29)	5471(15)	4324(10)
C(5)	7368(47)	7166(23)	4319(13)
C(6)	5220(24)	1206(18)	2726(8)
C(7)	6795(26)	798(12)	3863(9)
C(8)	6422(25)	1571(13)	3876(9)
C(9)	6993(25)	385(13)	4323(8)
C(10)	7052(32)	1925(14)	4387(11)
C(11)	−851(28)	3722(20)	1963(8)
C(12)	945(26)	3747(20)	1995(9)
C(13)	1808(24)	3695(16)	2519(8)
C(14)	−1773(29)	3787(23)	1427(9)
C(15)	−796(34)	3703(19)	921(10)
C(16)	−3557(29)	3724(26)	1399(9)
N(1)	−14(30)	3827(19)	489(9)
N(2)	−5054(28)	3842(13)	1383(10)

Cyclic voltammetry was performed in acetonitrile under a nitrogen atmosphere using 0.1 M tetrabutylammonium tetrafluoroborate (1 M=1 mol dm^{-3}) as a supporting electrolyte using Pt electrodes at a scan speed of 100 mV s^{-1}.

The temperature dependences of electrical resistivities were measured by a standard four-probe d.c. technique. The contacts were applied using gold paint with 20 μm gold wires. Measurements of the thermoelectric power along the a-axis was performed by attaching single crystals with 1 μm thick gold foils to two boron nitride heat sinks.[6] ESR data for a single crystal were obtained by an X-band spectrometer Varian E112 equipped with an Oxford Instruments ESR continuous-flow helium cryostat.

Results and Discussion

A cyclic voltammogram of $NMPy^+$ $AzaTCNQ^-$ in acetonitrile under a nitrogen atmosphere showed a redox wave ($AzaTCNQ^-/AzaTCNQ^{\cdot}$) with $E_{1/2}$=+0.57 V vs. SCE; ΔE^p=90 mV,[7] which is agreeable to that of $K^+AzaTCNQ^-$ ($E_{1/2}$=+0.54 V vs. SCE; ΔE^p=60 mV)[8] in acetonitrile. No second wave corresponding to $AzaTCNQ^{2-}/AzaTCNQ^-$ appeared. Furthermore, the reversible wave of $AzaTCNQ^{\cdot}/AzaTCNQ^+$ could not be obtained, although $AzaTCNQ^+$ has a similar electronic structure to TCNQ. The redox potential is close to those of $F_4TCNQ^{\cdot-}/F_4TCNQ$ ($E_{1/2}$=0.53 V vs. SCE; ΔE^p=59 mV) and $HCBD^{\cdot-}$/HCBD ($E_{1/2}$=0.62 V vs. SCE; ΔE^p=68 mV) obtained under the same conditions. From those data the order of acceptor strength is $F_4TCNQ<AzaTCNQ<HCBD$.

Usually, F_4TCNQ gives 1:1 insulating complexes with TTF derivatives in which both component molecules are completely charge-transfered and face-to-face segregated stacks are formed in the TTF, HMTTF, HMTSF, and DBTTF complexes,[9] while HCBD forms not only 1:1 complexes with perylene,[10] TMTTF,[11] and TTMTTF[11] but also 2:1 CT-complexes with pyrene,[12] hexamethylbenzene,[12] TTF,[13] and TMTTF.[11] The AzaTCNQ complexes form both 1:1 and 2:1 systems like the HCBD complexes. Though the chemical structure of AzaTCNQ resembles that of F_4TCNQ, the given complexes have more similar features to those of HCBD complexes.

Table 2. Electrical Properties of the AzaTCNQ Complexes

	ρ_{RT}/Ω cm	E_a/eV
TTF·AzaTCNQ[a]	66	0.20
$(TMTTF)_2AzaTCNQ$	8.1	0.072
$(TMTSF)_2AzaTCNQ$	1.1×10^{-2}	0.015 (at low temp)
DBTTF-AzaTCNQ[b]	19	0.09
HMTTF-AzaTCNQ[b]	1.3×10^6	—

a) A compacted sample. b) The stoichiometries have not been determined.

The electrical resistivities at room temperature and the activation energies of the AzaTCNQ complexes are summarized in Table 2. AzaTCNQ complexes with DBTTF, HMTTF, TMTTF, and TTF are semiconductors and only the TMTSF complex shows a metallic character (vide infra).

It is also noticeable that the electrical resistivity of the TTF complex is rather low, 66 Ω cm, at room temperature for the compacted sample, though it is a complete-charge-transfered salt with 1:1 stoichiometry(vide infra).[14] Our resistivity data agree with those of the Wudl's TTF complex. The appearance of the 1420 cm^{-1} band of C=C stretching and the 508 cm^{-1} band of C-S streching in TTF in the Raman spectrum suggests a complete charge transfer in this complex (cf. TTF^{+1} 1420 cm^{-1} (C=C), 509 cm^{-1} (C-S)).[15] This assignment was further confirmed by the optical absorption spectrum of a complex which does not show any absorption band in the near-infrared region, characteristic of a partial charge-transfer state. Unfortunately, the single crystals have not yet been obtained.

For the TMTSF complex, which shows a metallic character, a crystal structure analysis was performed. Weissenberg photographs and a four-circle diffractometer were employed to determine the crystal data of $(TMTSF)_2AzaTCNQ$: monoclinic, space group $C2/c$, a=7.738(1), b=19.531(2), c=23.146(3) Å, β=90.03(1)°, V=3498.3(8) $Å^3$, and Z=4. The a-axis corresponds to the crystal needle axis. The oscillation photograph along the a-axis displayed strong, even layer lines due to the two-fold periodicity of the donors. All these layer lines were composed of well-defined spots, even at room temperature, and no diffuse track was observed. The crystal structure is illustrated in Figs. 2—4. The planar TMTSF molecules form face-to-face one-dimensional stacks along the a-axis with an interplanar spacing of 3.6 Å, which corresponds to a conduction column (Fig. 4). Within the one-dimensional

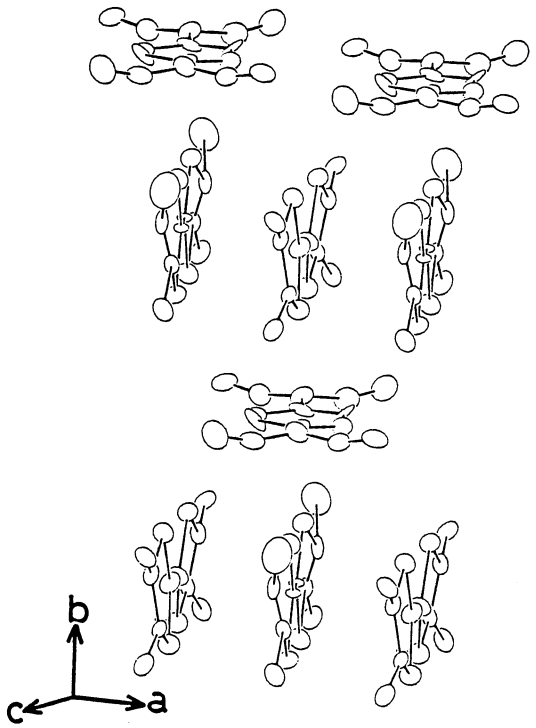

Fig. 2. Molecular arrangement of $(TMTSF)_2$ AzaTCNQ viewed along nearly the long axis of the donor molecule.

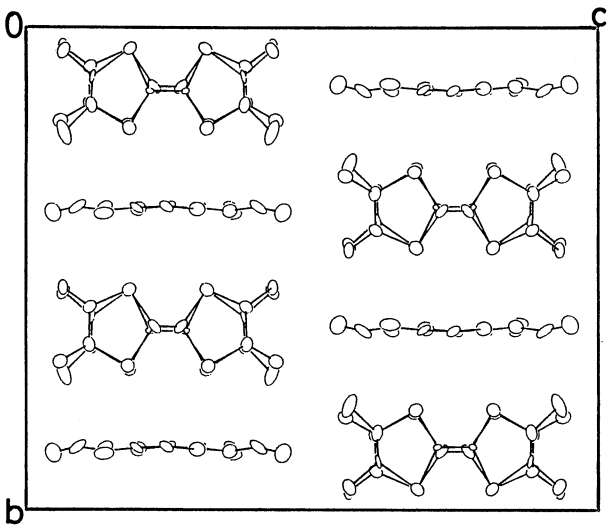

Fig. 3. Crystal structure of $(TMTSF)_2$AzaTCNQ projected along the axis perpendicular to the (100) plane.

stacks the Se···Se distances between the neighboring TMTSF molecules are 3.72—4.02 Å, which are comparable to twice the van der Waals radii of Se···Se, 3.80 Å. On the other hand, the AzaTCNQ molecular planes are arranged side-by-side along the donor stacks and the acceptor molecules surround the TMTSF columns so that the donor stacks are isolated from each other. There are no short atomic contacts between the neighboring donor columns; hence, the molecules form nearly complete one-dimensional stacks, as can

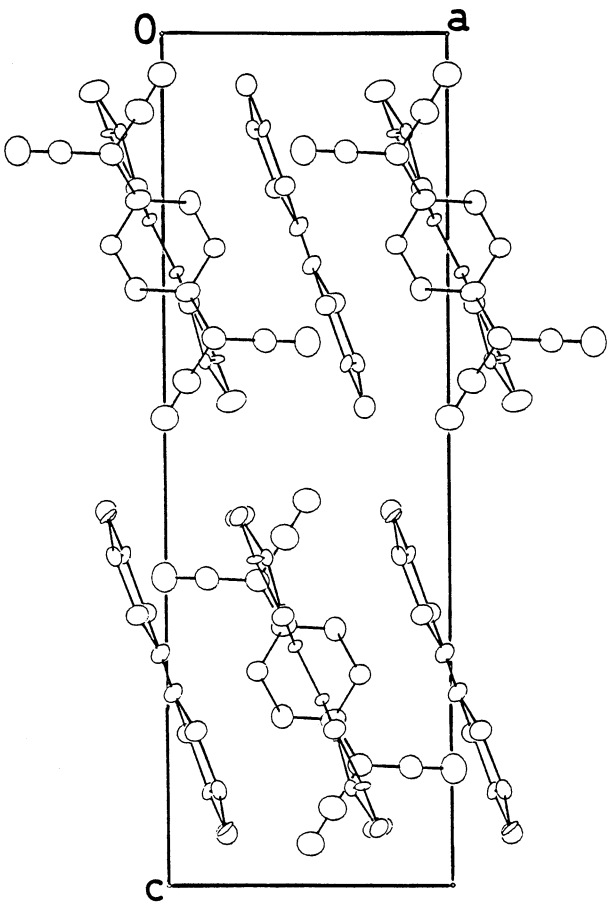

Fig. 4. Crystal structure of $(TMTSF)_2$AzaTCNQ projected along the b axis.

be seen in Fig. 3. The dihedral angle between the least-square planes of donor and acceptor molecules is 93° (Fig. 4). The AzaTCNQ molecules are oriented parallel to the ac plane, while the longitudinal axes of TMTSF molecules are tilted by approximately 20° from the [001] direction (Fig. 4).

Another remarkable feature is that the orientation of AzaTCNQ molecules has a disorder in nature. There appears a two-fold axis through the center of every AzaTCNQ molecule, so that the nitrogen atom in the pyridine skeleton of each AzaTCNQ molecule is randomly located at either position of two equivalent sites.

$(TMTTF)_2$AzaTCNQ is essentially isomorphous with the TMTSF complex. The crystal data are: monoclinic, space group $C2/c$, a=7.670(3), b=19.178(9), c=22.655(3) Å, β=90.25(2)°, V=3332.3(22) Å^3, and Z=4.

These structures have some similarities to that of $(TMTTF)_2$HCBD,[11b] in which the orientationally disordered acceptors lie almost perpendicular to the donor planes and surround the donors, showing one-dimensionality characteristics. A slight difference between $(TMTTF)_2$HCBD and $(TMTTF)_2$AzaTCNQ is that the donors in the HCBD complex stack in a dimerized manner with a molecular separation of ca. 3.5 Å within the dimer and ca. 3.7 Å between the

dimers. The HCBD complex is a semiconductor (ρ_{RT}=3.3×10^3 Ω cm, E_a=0.16 eV). As for (TMTTF)$_2$ AzaTCNQ, the electrical resistivity and the activation energy are lower than those of (TMTTF)$_2$HCBD. This may be caused by the uniform stacking of donors in (TMTTF)$_2$AzaTCNQ, where the interplanar spacing of 3.5 Å was observed.

A substitution of the selenium for sulfur atoms of donors may cause less on-site Coulomb repulsions and stronger intermolecular interactions between donors and influence the charge transport. As a consequence, (TMTSF)$_2$AzaTCNQ with uniform stackings shows a metallic character down to 200 K, as illustrated in Fig. 5. Upon lowering the temperature to below 150 K the resistivity gradually increases and is activated with a very small activation energy of E_a=0.015 eV.

The result of thermoelectric power (S) measurements shows positive values due to the hole conduction, which is consistent with the conducting paths of donors in the crystal (Fig. 6). The thermoelectric power linearly falls with decreasing temperature and the extrapolation tends to approach zero at 0 K, suggesting a metallic state above 150 K. The transition temperature is a little lower than that of the electrical resistivity. The higher transition temperature of the electrical resistivity may be caused by a strong sensitivity to the influence of the random potential originating from the orientational disorder of AzaTCNQ molecules. Assuming a simple one-electron tight-binding band model, the thermoelectric power along the conducting axis can be written as

$$S = \frac{-\pi^2 k_B^2 T}{6|e|t} \cdot \frac{\cos(\pi\rho/2)}{1-\cos^2(\pi\rho/2)},$$

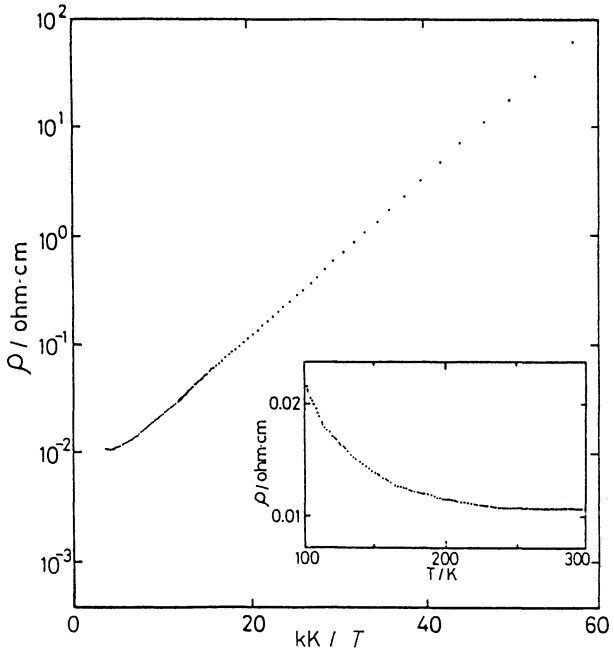

Fig. 5. Temperature dependence of the electrical resistivity of (TMTSF)$_2$AzaTCNQ along the a axis.

where e is the electron charge, k_B is the Boltzmann constant, and ρ is the electron density (in our case ρ=2−1/2=3/2).[16] From the slope of S vs. T plots at high temperatures, the transfer integral(t) was obtained as 0.25 eV ($4t$=1.0 eV). Below the metal-semiconductor transition, S gradually increases. For a simple semiconductor, the thermoelectric power can be described as

$$S = \text{constant} - \frac{k_B}{e} \cdot \frac{b-1}{b+1} \cdot \frac{E_g}{2k_B} \cdot \frac{1}{T},$$

where E_g is the energy gap and $b=\mu_e/\mu_h$, i.e., the ratio of an electron to a hole mobility.[16] From the positive values of the thermoelectric power and the one-dimensional conduction pathways composed of the only donor component shown by the crystal structure analysis, $-(b-1/b+1)$ can be regarded as 1. The activation energy was found to be E_a=0.018 eV from the slope of S vs. $1/T$ plots below 55 K. This value of the activation energy is in a good agreement with the derived value from the electrical conductivity.

Only one signal of the ESR spectra of (TMTSF)$_2$-AzaTCNQ has been observed and the line shape was found to be Lorentzian all the way down to 34 K. The

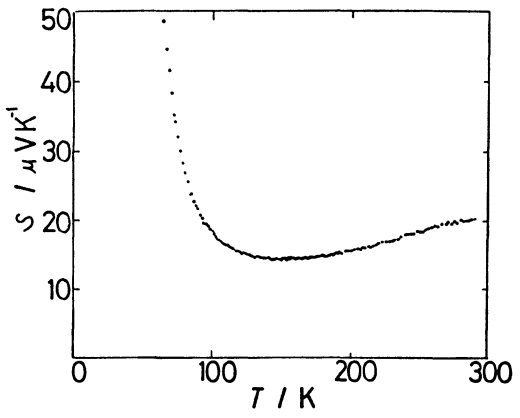

Fig. 6. Temperature dependence of the thermoelectric power S of (TMTSF)$_2$AzaTCNQ along the a axis.

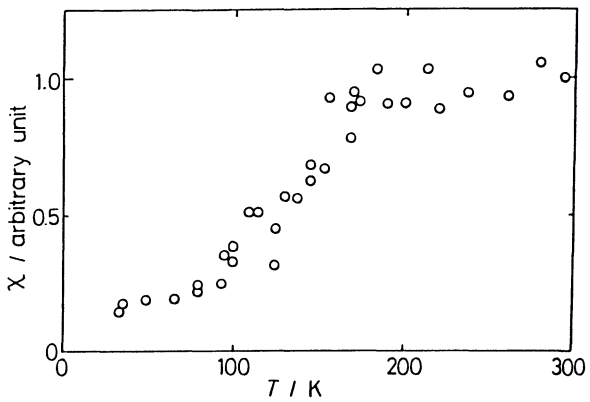

Fig. 7. Temperature dependence of the ESR magnetic susceptibility of (TMTSF)$_2$AzaTCNQ.

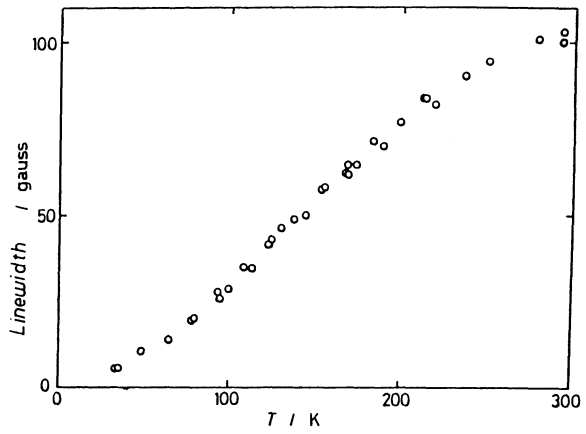

Fig. 8. Temperature dependence of the ESR linewidth of $(TMTSF)_2AzaTCNQ$.

magnetic susceptibility obtained from the ESR intensity of $(TMTSF)_2AzaTCNQ$ is almost constant, indicating a Pauli-like paramagnetism above 150 K (Fig. 7). Below that temperature the susceptibility behaves in an activated manner with E_a=0.03 eV. This value agrees fairly well with those of the electrical resistivity and thermoelectric power. Judging from the charge-transport and magnetic properties, a metal-semiconductor transition is considered to occur at ca. 150 K. It is regarded as being the Peierls transition.

Figure 8 illustrates the temperature dependence of the ESR line width for the applied field H_0 approximately parallel to the a-axis. The line width (ΔH) at 293 K is almost 95 G (1G=10^{-4} T) which is a little narrower than those of $(TMTSF)_2X$ (X=PF_6, BF_4, NO_3, and etc. ΔH>150 G),[17] suggesting a lower dimensionality of the AzaTCNQ complex than those of $(TMTSF)_2X$. Below room temperature the width decrease approximately linearly with the temperature down to about 250 K, below which the temperature dependence becomes stronger and the width decrease linearly to 5 G at 34 K. The temperature dependences are reminiscent of those of single-chain conducting complexes $(TMTSF)_2X$, which show knees at a little bit lower temperature (100—180 K) than that of the AzaTCNQ complex. The anisotoropy in the linewidth becomes smaller as the temperature becomes lower (ΔH=28 G (*//a*), 36 G (*//b*) at 99 K and 95 G (*//a*), 127 G (*//b*) at 293 K). The line width of the AzaTCNQ complex shows no drastic behavior in the temperature region of the metal-semiconductor trasition, which may indicate a gradual transition of this complex due to the orientational disorder of AzaTCNQ molecules.

The angular dependence of the *g* values is similar to that of the linewidth. The *g* values are usually different in the direction of the applied H_0 to the donor molecules. The maximum, intermediate, and minimum *g* values are generally found when H_0 is applied to a long axis, a short axis and perpendicular to a molecular plane, respectively. The observed *g*-value is

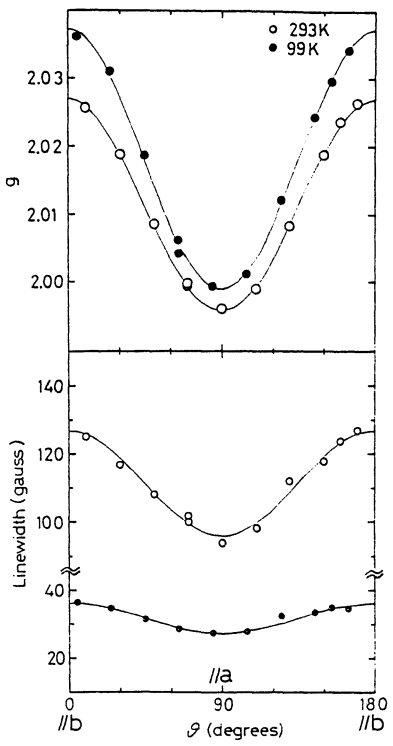

Fig. 9. Angular dependences of the *g* values and linewidth of $(TMTSF)_2AzaTCNQ$ at 293 and 99 K.

intermediate when H_0 is parallel to the b-axis (g_{int} ca. 2.026), which is approximately parallel to the short axis of the TMTSF molecules in the crystal. However, the minimum *g*-value is observed for H_0 parallel to the a-axis (g_{min} ca. 1.996), which is nearly normal to the molecular plane of TMTSF and, hence, along the conducting direction. Those values compare well to those of $(TMTSF)_2PF_6$ (g_{int} ca. 2.027, g_{min} ca. 1.989), strongly suggesting that AzaTCNQ behaves as a closed-shell counter anion. The anisotropy of the *g*-values is in good accordance with those previously reported ones in $(TMTSF)_2X$[18,19] and $(BEDT\text{-}TTF)_2X$[19] in that the intermediate *g*-value corresponds to the short axis of the donor molecule and the minimum *g* is perpendicular to the molecular plane. More precise anisotropy studies of the line width and the *g*-values of the AzaTCNQ complex are presently being carried out.

In summary, AzaTCNQ has been found to form conducting organic compounds with TTF derivatives. Among them $(TMTSF)_2AzaTCNQ$, in which AzaTCNQ most likely acts as a closed-shell counter anion, is the most conductive and the transport properties indicate its metallic character down to 150 K, where the Peierls-type instability takes place.

The authors wish to express their thanks to Professor Gen-etsu Matsubayashi of Osaka University for his valuable advice concerning the synthesis and Mr. Kenichi Imaeda for his helpful advice concerning electrical and ESR measurements.

References

1) Abbreviations for compounds: TTF, tetrathiafulvalene; TMTTF, tetramethyltetrathiafulvalene; TMTSF, tetramethyltetraselenafulvalene; HMTTF, hexamethylenetetrathiafulvalene; DBTTF, dibenzotetrathiafulvalene.

2) F. Wudl, "Chemistry and Physics of One-dimensional Metals," ed. by H. J. Keller, NATO Adv. Study Inst., (1977), p. 249.

3) H. Tanaka, G. Matsubayashi, and T. Tanaka, *Bull. Chem. Soc. Jpn.*, **57**, 2198 (1984).

4) H. Urayama, T. Inabe, T. Mori, Y. Maruyama, G. Saito, *Synth. Metals*, **19**, 469 (1987).

5) "International Tables for X-ray Crystallography," Kynoch Press, Birmingham (1974), Vol. IV.

6) P. M. Chaikin and J .F. Kwak, *Rev. Sci. Instrum*, **46**, 218 (1975).

7) ΔE^{p} is defined as the difference between the cathodic and anodic peak potentials.

8) G. Matsubayashi, H. Tanaka, T. Tanaka, and K. Nakatsu, *Inorg. Chim. Acta*, **63**, 217 (1982).

9) a) F. M. Wiygul, T. J. Emge, and T. J. Kistenmacher, *Mol. Cryst. Liq. Cryst.*, **90**, 163 (1982); b) J. B. Torrance, J. J. Mayerle, K. Bechgaard, B. D. Silverman, and Y. Tomkiewicz, *Phys. Rev. B*, **22**, 4960 (1980); c) M. E. Hawley, T. O. Poehler, T. F. Carruthers, A. N. Bloch, D. O. Cowan, and T. J. Kistenmacher, *Bull. Am. Phys. Soc.*, **23**, 424 (1978); d) T. J. Emge, W. A. Bryden, F. M. Wiygul, D. O. Cowan, T. J. Kistenmacher, and A. N. Bloch, *J. Chem. Phys.*, **77**, 3188 (1982).

10) H. Yamochi, G. Saito, T. Sugano, M. Kinoshita, C. Katayama, and J. Tanaka, *Chem. Lett.*, **1986**, 1303.

11) a) G. Saito, T. Enoki, H. Inokuchi, H. Kumagai, C. Katayama, and J. Tanaka, *Mol. Cryst. Liq. Cryst.*, **120**, 345 (1985); b) C. Katayama, M. Honda, H. Kumagai, J. Tanaka, G. Saito, and H. Inokuchi, *Bull. Chem. Soc. Jpn.*, **58**, 2272 (1985).

12) O. W. Webster, *J. Am. Chem. Soc.*, **86**, 2898 (1864).

13) F. Wudl and E. W. Southwick, *J. Chem. Soc., Chem. Commun.*, **1974**, 254.

14) Found: S, 30.85; C, 49.02; N, 16.49; H, 1.92%. Calcd for $S_8C_{23}N_5H_{12}$; S, 31.24; C, 49.74; N, 17.06; H, 1.96%.

15) a) Unpublished data by Prof. S. Matsuzaki; b) S. Matsuzaki, T. Moriyama, and K. Toyoda, *Solid State Commun.*, **34**, 857 (1980).

16) P. M. Chaikin, R. L. Greene, S. Etemad, and E. Engler, *Phys. Rev. B*, **13**, 1627 (1976).

17) H. J. Pedersen, J. C. Scott, and K. Bechgaard, *Phys. Rev. B*, **24**, 5014 (1981).

18) N. Kinoshita, M. Tokumoto, H. Anzai, T. Ishiguro, G. Saito, T. Yamabe, and H. Teramae, *J. Phys. Soc. Jpn.*, **53**, 1504 (1984).

19) T. Sugano, G. Saito, and M. Kinoshita, *Phys. Rev. B*, **34**, 117 (1986).